High Efficiency Amine Functionalization of Cyclo Olefin Polymer Surfaces for Biodiagnostics.

Ram P. Gandhiraman*[a], Cedric Volcke[b], Vladimir Gubala[a], Colin Doyle[c], Lourdes Basabe-Desmonts[a], Christian Dotzler[d,e], Michael F. Toney[e], Marcello Iacono[a], Robert I. Nooney[a], Stephen Daniels[a,f], Bryony James[c] and David E. Williams[g]

Received (in XXX, XXX) Xth XXXXXXXXX 200X, Accepted Xth XXXXXXXXX 200X
First published on the web Xth XXXXXXXXX 200X
DOI: 10.1039/b000000x

Point-of-care diagnostics (POC) implementing microfluidic technology on single use disposable plastic chips has potential applications in personalized medicine, clinical diagnostics and global health. However, the challenges in commercializing POC devices must be addressed. Immobilization of biomolecules to plastic chips through appropriate surface functionalization is a key issue for the fabrication of new generation biomedical diagnostic devices. The most important requirements for a practicable surface functionalization process are speed, control and reliability. Plasma-based methods can meet these criteria. A single step, solventless, ecofriendly and high throughput nature of plasma processing make them highly attractive. Here we demonstrate the efficient surface functionalization of a next-generation biosensor material, a chemically-inert cyclo olefin polymer (COP). The plasma formation of a surface-bound aminated siloxane network from mixed aminopropyltriethoxy silane and ethylene diamine precursors allowed us to form a well-adherent film with an exceptionally high degree of amine functionalization. We deduce that the siloxane was the critical component for radical insertion into the COP and for building a stable network to support the reactive amine functionalities. We present a full physical and chemical characterization of the films, including a detailed study of their swelling in water, using an array of surface analytical techniques: X-ray photoelectron spectroscopy, X-ray reflectivity, reflection infra-red spectroscopy, atomic force microscopy (AFM) and fluorophore binding reactions. We demonstrate an original approach for qualitatively analyzing the distribution of amine functionalities by counting surface-bound functionalized silica nanoparticles in the AFM. The relative contributions from covalent (specific) and non-covalent (non-specific) reaction chemistry assessed using 3'-fluorescein-labeled ssDNA attachment showed that the non-specific binding could be reduced significantly according to the particular feed gas mixture used to prepare the coating. A reaction mechanism has been proposed for the deposition of amine functionalities on COP plastic and also for enhancing the amine functionalities that affects the non specific binding significantly.

Introduction

There is intense effort directed at the development of polymer based devices implementing microfluidics for new generation biosensors and biomedical diagnostic devices. A number of concepts have been demonstrated to implement the necessary fluid handling and metering.[1] However, immobilization of the biorecognition reagents to the polymer surface in a rapid, repeatable and controllable fashion remains a key challenge. For a biosensor to work efficiently, biomolecules have to be immobilized on surfaces in their biologically active state with low non-specific binding. A number of methods have been described for this. In normal laboratory and commercial practice, a simple chemisorption of the active reagents onto the sensor surface is commonly employed, since the method is inexpensive and rapid.[2,3] A variety of reactive surface binding techniques have also been described in the literature, generally aimed at improving the surface binding activity by appropriate functionalization of the surface.[4-7] Amine functionalization of the biosensor device platform can enable covalent immobilization of biomolecules. Such solution-based multi-step procedures are complicated, time-consuming and in general not appropriate for large-scale production.

The performance of new polymeric materials has led the biomedical diagnostics industry to develop cheap disposable biosensor platforms, appropriate for point-of-care applications. Zeonor®, a type of cycloolefin polymer (COP), is one such polymer presenting excellent optical properties, good chemical resistance, ease of fabrication and cost effectiveness.[8,9] It is, however, chemically inert and so there are two issues that are very significant with respect to the practical development of devices utilizing COP polymers as

substrates. The first is how to achieve a suitably reactive surface for functionalization. The second is how to prepare a suitably reactive and stable surface with a sufficiently rapid, repeatable and controllable process. It is this point that we address in this paper: we demonstrate a plasma polymerization route to a stable, amine-functionalized surface on COP and thoroughly characterize the resultant surface layer with respect to its thickness, adhesion, swelling in water, chemical composition, functional reactivity and use as a sensor platform.

In recent literature, surface activation of COP by the use of an oxygen plasma or by treatment in ozone under UV light has been demonstrated.[10-12] Liquid-phase treatments with aminosilanes to create surfaces that are reactive towards antibodies and other specific binding molecules have been extensively investigated.[13-16] However, much care and attention to detail is needed to control the water content of the treatment solutions and the degree of surface hydroxylation in order to obtain reproducible surface conditions.[15-16] These multi-step procedure involves activation of the substrate by oxygen plasma, transfer of samples from plasma chamber to liquid container and also handling of liquid wastes. Gas-phase deposition overcomes these drawbacks.[17-20] However, most published investigations have concerned the simple vapour-phase reaction of aminosilanes with an hydroxylated surface, usually glass or silicon at high temperatures that are not suitable for COP chips.[21,22] In contrast to the multi-step complexity of the methods described above, we have found that a fast and simple route to versatile amine-functionalized surfaces on COP plastics is to combine the oxygen plasma activation method with plasma enhanced chemical vapour deposition (PECVD) from an aminated precursor. PECVD, a single step high throughput process, is a versatile surface engineering technique which has proven to be an excellent tool for surface modification and large scale production that does not leave behind liquid waste.[23,24] PECVD enables rapid, low-temperature deposition of diverse functional groups in a controlled manner. In this technique, a plasma discharge is created in presence of a precursor containing the required chemical group. The deposited coatings are uniformly dispersed with a precisely controlled thickness. The characteristics of the coating are highly dependent on the nature of the substrate, precursor and plasma process parameters, particularly the applied input power and deposition time.[25,26] Surface amination by PECVD has previously been demonstrated from ethylene diamine (EDA) precursor on glass and titanium.[26-28] An alternative precursor for amine functionalization on COP surfaces is 3- amino propyltriethoxy silane (APTES) : it is known that siloxane PECVD precursors give a well-adherent silica-like layer on COP 29,30 so the presence of Si-O groups in APTES could be expected to create chemical bonding to the plasma-activated COP surface and to provide a network to build the layer, allowing a good adhesion and stability of the coating. The amino functionality is expected to be retained with appropriate choice of plasma parameters, thus providing the required reactivity.

With the objective of creating adherent, reactive amino-functionalised coatings on COP we explored the PECVD approach with the different amino precursors: ethylene diamine (EDA) and APTES. Using these two precursors we evaluated the effect of the presence of the SiOR group. We also explored the codeposition of these two precursors to create high density amino coatings on COP by PECVD. The chemical and physical characterization of the plasma deposited coatings was performed using a multi-technique approach: X-ray photoelectron spectroscopy (XPS), X-ray reflectivity (XRR), Attenuated total reflectance Fourier transform infrared spectroscopy (ATR-FTIR), amine reactive fluorophore reaction, contact angle analysis and atomic force microscopy (AFM). A novel approach for qualitatively analyzing the homogeneity of amine groups on COP surface, by reactively coupling functionalized silica nanoparticles (NP) to the surface then counting the bound particles by AFM, is demonstrated. Biosensor application, and the control of non-specific binding through alteration of the composition of the coating is demonstrated through DNA attachment experiments .

Experimental details

Materials

Bare COP slides (Zeonor® 1060R) 75 mm x 25 mm were obtained from Åmic AB (Uppsala, Sweden). 3-aminopropyltriethoxysilane (APTES), ethylenediamine (EDA), phenyl diisothiocyanate (PDITC), acetonitrile and triethylamine were purchased from Sigma Aldrich and used without further treatment. Lissamine™ rhodamine B sulfonyl chloride (λexc. = 532 nm and λem = 550 nm) was obtained from Invitrogen. Sulfosuccinimidyl-4-[2-(4,4-dimethoxytrityl)]butyrate (sSDTB) was obtained from ProChem, Inc., and ssDNA from MWG Biotech

Plasma enhanced chemical vapor deposition (PECVD)

The deposition of amine functional coatings was carried out in a computer controlled PECVD reactor Europlasma, model CD300 (Oudenaarde, Ghent, Belgium). An aluminum vacuum chamber, connected to a Dressler CESAR 136 RF power source (Munsterau, Stolberg, Germany) with an operating frequency of 13.56 MHz, with an automated impedance-matching box, was used. The details of the deposition system is provided elsewhere.[31] The bare COP slides, 75 mm x 25 mm, were cleaned with dry air and then loaded in the chamber. The chamber was pumped to a base pressure of 20 mTorr. Prior to the deposition, plasma cleaning and activation was carried out using argon (50 sccm) + oxygen (50 sccm) mix plasma (250 watt RF power). After three minutes, the oxygen flow was closed and the RF power reduced to 14 watt. A needle valve, connected to the vacuum chamber, was used to control the flow of precursor vapors: APTES and EDA. The precursors were stored in two different containers and mixed in the plasma chamber. As the vapor pressure of APTES is

less than 10 Torr at 100° C, the APTES container was heated at 80° C and to prevent condensation of APTES in pipelines; the stainless steel supply lines from source to vacuum chamber were also heated at 80° C through a temperature controlled heating tape. The vapor pressure of EDA is 10 Torr at 20° C and hence no external heating was required at the operating pressure (~ 80 mTorr for APTES and ~ 100 mTorr for EDA). The deposition time was 4 minutes for all the coatings. The slides coated with APTES precursor alone are referred to as 'APTES coating' hereafter, the slides coated with EDA precursor alone are referred to as 'EDA coating' and the films co-deposited with APTES and EDA precursor are referred to as 'APTES+EDA'.

X-ray photoelectron spectroscopy (XPS)

The XPS data were collected on a Kratos Axis UltraDLD equipped with a hemispherical electron energy analyzer. Spectra were excited using monochromatic Al Kα X-rays (1486.69 eV) with the X-ray source operating at 100 W. This instrument illuminates a large area on the surface and then using hybrid magnetic and electrostatic lenses collects photoelectrons from a desired location on the surface. In this case the analysis area was a 220 by 220 micron spot. The measurements were carried out in a normal emission geometry. A charge neutralization system was used to alleviate sample charge buildup, resulting in a shift of approximately 3 eV to lower binding energy. Survey scans were collected with 160 eV pass energy, whilst core level scans were collected with pass energy of 20 eV. The analysis chamber was at pressures in the 10^{-9} Torr range throughout the data collection.

Data analysis was performed using CasaXPS (www.casaXPS.com). Shirley backgrounds were used in the peak fitting. Quantification of survey scans utilised relative sensitivity factors supplied with the instrument. Core level data were fitted using Gaussian-Lorentzian peaks (30 % Lorentzian). The binding energy scale was corrected for the neutraliser shift by using the C 1s signal from saturated hydrocarbon at 285.0 eV as an internal standard.

Colorimetric assay

For quantification of amine groups by colorimetric method, reaction with sulfosuccinimidyl-4-[2-(4,4-dimethoxytrityl)]butyrate (sSDTB), was used. Briefly, two sets of amino coated substrates were prepared. One set of the substrates was pre-treated by ultrasonication in a 1 % solution by weight of sodium dodecyl sulfate (SDS), while the other set was not so treated. All substrates were then immersed in a freshly prepared solution of sSDTB (0.1 mM at pH = 8.0) for 30 minutes at room temperature. After incubation, all substrates were thoroughly rinsed with water and then treated with a 37.5 % perchloric acid to allow the formation of 4,4'-dimethoxytrityl cation from the substrates. Since the reaction between the amines and the sSDTB proceeds with 1:1 stoichiometric ratio, the concentration of the released cation measured by UV/vis spectrophotometer at 498 nm was used to quantify the amine group density.

Lissamine fluorophore attachment

Fluorophore attachment to amino-functionalized Zeonor® substrates was achieved by spotting onto the sample coated slides 0.2 µl of 2.5 10-7 M lissamine™ rhodamine B sulfonyl chloride in DMF/H2O (10:33) and incubated for 30 minutes. . One sample from each batch was ultrasonicated in water, another batch was ultrasonicated in SDS and a third batch was ultrasonicated in PBS Tween for 1 minute and the fluorescence intensity was measured using a GMS 418 plate scanner (Genetic Microsystems, Affymetrix). The samples were again ultrasonicated separately in water, SDS and PBS-Tween and the fluorescence intensity was measured. This process was repeated 6 times.

Attenuated total reflection – Fourier transform infrared spectroscopy (ATR-FTIR)

The nature of chemical bonding present in the film is determined by a Fourier-transform infrared spectroscopy system (Perkin Elmer – Spectrum GX FTIR) used in the attenuated total reflection (ATR) mode (Horizontal accessory equipped with a ZnSe crystal, Perkin Elmer). The detector and the sample chamber were filled with nitrogen gas during measurements. For all data presented, unmodified Zeonor slides were used as background.

Nanoparticle synthesis and conjugation to functionalized COP substrates

Silica nanoparticles (NP) were prepared using a microemulsion method.[32] The microemulsion was formed by adding water (0.96 ml) to a mixture of cyclohexane (15 ml), n-hexanol (3.6 ml) and Triton® X-100 (3.788 g). Following this tetraethylorthosilicate (TEOS) (0.2 ml) and NH4OH (0.16 ml) were added to start the growth of the silica NPs. The reaction was stirred for 24 hrs, after which TEOS (0.1 ml) was added with rapid stirring. After 30 minutes 3-trihydroxysilylpropylmethylphosphonate, sodium salt THPMP (0.08 ml) was added with stirring to prevent aggregation of the nanoparticles. After a further 5 minutes 3-aminopropyltrimethoxysilane (APTMS) (0.02 ml) was added for conjugation to the amine functionalized surfaces. The NPs were separated from the solution with the addition of excess absolute ethanol and centrifuged twice with ethanol and once with deionized water (Heraeus, Biofuge pico). Sonication was used between the washing steps to resuspend the NPs. The NPs were dispersed in deionized water, at 2.0 mg / ml and stored in the dark at 4° C.

The plain COP slides and microfluidic chips coated with amine groups were first dipped in an aqueous solution containing glutaraldehyde (2 wt %) for 24 hours. Following this the slides were dipped in an aqueous solution containing NPs (2.0 mg / ml) for a further 24 hours. The amount of surface coverage was determined using atomic force microscopy (AFM). The schematic for NP attachment to

functionalised COP substrate is shown in **Fig. 1.**

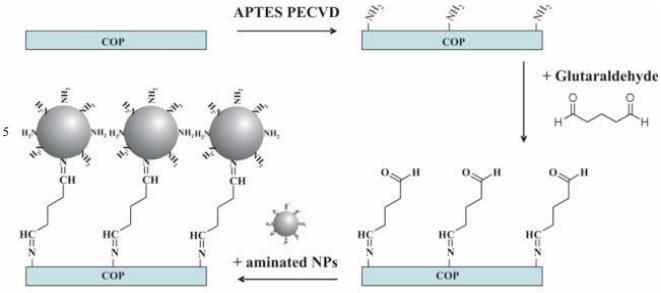

Figure 1. Scheme presenting the original nanoparticle approach developed. The plasma deposited amino coated COP surfaces are dipped in a glutaraldehyde solution (2 wt %) for 24 hrs and then in dipped in an aqueous solution containing amino functionalized silica nanoparticles (2.0 mg / ml) for a further 24 hrs.

Atomic force microscopy (AFM)

AFM examinations were performed with a commercial AFM (Dimension 3100 AFM using a Nanoscope IIIa controller equipped with a phase imaging extender, Digital Instruments) operating in tapping-mode™ (TM-AFM), using standard silicon tips (Tap300Al, BudgetSensors,) with 42 N/m nominal spring constant and 300 kHz nominal resonance frequency. The images were flattened using second-order flattening routines to remove any sample tilt and/or curvature before obtaining root-mean-square (rms) roughness values. No further filtering was performed. Roughness values presented are averaged values obtained from three different measurements on 1 µm x 1 µm images.

X-ray reflectivity (XRR)

X-ray reflectivity was used to investigate water uptake of the functionalized films.[33] Measurements were performed at the Stanford Synchrotron Radiation Light Source (SSRL) on the thin film diffraction beam line 2-1, equipped with a Huber 2-circle goniometer. X-rays of 1.55 Å were monochromated with a Si(111) double-crystal. Reflected X-rays were collimated by a pair of 1 mm slits and detected with a Bicron NaI detector. The reflectivity is defined as the ratio of reflected and incident beam and is measured as a function of the z-component of the momentum transfer $q = (4\pi/\lambda)\sin(2\theta/2)$, which is normal to the sample surface. The diffuse scattering component was measured with offset incidence angles $2\theta/2 \pm 0.1°$ and was subtracted from the specular reflectivity with incidence angle $2\theta/2$. The measured reflectivity gives information on the variation of the scattering length density (SLD) normal to the sample surface. Model dependent fits of the reflectivity profile, assuming a multilayer structure parameterized by layer thickness and root mean square (rms) roughness values, were performed using the Abeles matrix method[34] implemented in the MOTOFIT analysis package.[35]

In order to obtain the smooth sample surface necessary for reflectivity measurements, COP was spin coated on silicon (111) substrates. For spin coating, Zeonor® pellets were first oven-dried at 60° C for 4 hours and then dissolved in xylene to a concentration of about 2.5 g / l. The solution was then ultrasonicated for 10 minutes and filtered with 0.45 µm pore filter paper to filter out undissolved aggregates. It was then spin coated on silicon. The thickness of the COP layer is estimated as 70 Å, as determined from ellipsometry measurements. For the XRR measurements, the samples were placed in a sealed sample chamber with Kapton windows for controlled atmosphere. During the measurements, the sample chamber was either flushed with dry N_2 or with water vapour by bubbling dry N_2 through a water reservoir.

DNA attachment

The APTES and APTES+EDA coated slides were incubated with 1,4-phenyldiisothiocyanate (PDITC) in DMF : pyridine mixture (9:1) for 2 hours to create an amino-reactive site. The slides were then washed with DMF, MeOH and dried under stream of N_2. One set of such PDITC activated slides was subsequently blocked in blocking buffer (containing 5mM of H2N-PEG4-COOH) for 4 hours. Afterwards, ssDNA modified at 5'-terminal with amino modifier and 3'-terminus with FITC was diluted in printing buffer (10% glycerol, 0.1 M sodium citrate at pH=8.5) and micro spotted (50 drops, 0.6 nL each) onto both the PDITC activated slide and the blocked slide using a microarray spotter. The coupling reaction was allowed to proceed for 4 hours at 25°C in a humid chamber. The arrayed slides were then washed with 0.1% SDS followed by extensive wash with DI water.

Results and discussion

Quantitative analysis by XPS and colorimetric experiment using sSDTB

X-ray photoelectron spectroscopy (XPS) was carried out for a quantitative elemental analysis of the plasma deposited coatings. To study the various bonding environments, a high resolution scan for the core level photoemission spectra of C 1s peak was carried out. The elements present in the three coatings, EDA, APTES and APTES + EDA (C, O, Si and N) were identified from XPS survey spectra (see Supporting Information). For further analysis, high-resolution spectra were recorded from individual peaks.

Sample	C 1s peak		At % in the sample
Zeonor®	Binding Energy (eV)	Attribution	C - 98.5, O - 1.1 Si - 0.4
	285.0 (84 %) 285.9 (13.9 %) 287.5 (2.1 %)	C-C Vibrational component of C-C. Surface oxide	
EDA	285.0 (45.2 %) 286.6 (36.5 %) 288.6 (18.3 %)	C-C C-N CONH2	C - 64.9, Cl - 0.2 N -15.2, O - 17.1 Si - 2.4, S - 0.2
APTES	285 (51.7 %) 286.4 (36 %) 288.4 (12.3 %)	C-C C-N CONH2	C - 49.0, N - 5.8 O - 30.7, Si - 14.5
APTES+EDA	285.0 (44.1 %) 286.4 (41.7 %) 288.5 (14.2 %)	C-C C-N CONH2	C - 49.6, Cl - 0.8 N - 8.6, O - 29.8 Si - 11.1

Table 1 Elemental analysis by XPS

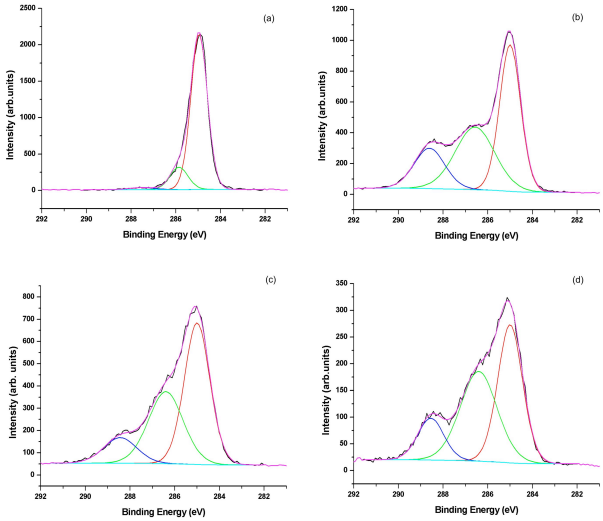

Figure 2. High resolution C 1s core level photoemission spectra of (a) untreated COP surface, (b) EDA (c) APTES and (d) APTES+EDA coating on COP substrates, taken with a pass energy of 20 eV using monochromatic Al Kα monochromatic X-rays. The C 1s peak is deconvoluted to show the various bonding environments in carbon.

Qualitatively the C 1s spectra for all coatings (**Fig. 2.**) look reasonably similar with a saturated hydrocarbon peak (285.0 eV) and two additional peaks to higher binding energy at 286.4 eV (~ +1.4) and 288.4 eV (~ +3.4), which are best associated to C-N bonding and –CONH2 groups, respectively. The deconvoluted C 1s spectrum of the plain COP substrate (**Fig. 2(a)**) shows an additional peak at 285.8 eV along with the major C-C peak. This peak is included to account for peak asymmetry due to vibrational fine structure in the C-C component, which could also have been fitted using either a vibrational progression, or an asymmetric lineshape.[36]

In the case of C 1s spectra, the relative amount of C-N bonding is higher in APTES+EDA coating (41.7 %) than either the APTES (36 %) or EDA (36.5 %) coatings on their own (Table. 1). The $–CONH_2$ peak was most intense for the EDA coating (18.3%), less so for the APTES+EDA coating (14.2 %) and least for the APTES coating (12.2 %). Similarly, the elemental composition analysis revealed that the atomic percentage of nitrogen (N 1s) was higher for the EDA coating (15.2 %) than for the APTES+EDA (8.6 %) and APTES (5.8 %) coatings (**Table. 1**).

To determine the number of the free amino groups available for binding to an appropriate linker, a colorimetric method[37] based on the reaction between the free amines and a sulfosuccinimidyl-4-[2-(4,4-dimethoxytrityl)]butyrate (sSDTB), was employed (see Table 2). APTES+EDA coatings revealed a three times higher amount of reactive amino groups than either the EDA or APTES coatings. Moreover, when a pre-treatment, consisting of an ultrasonication in a 1 weight % SDS solution was applied to the coated samples, the number of reactive amino groups per cm² decreased sharply on for the EDA coated slides. In contrast, the number of reactive amino groups per cm² measured for the APTES and APTES+EDA coatings remained essentially unchanged after the detergent sonication procedure. This observation can be interpreted as a very poor adhesion of the EDA coating on COP substrates. Overall, the colorimetric measurement using sSDTB showed that APTES + EDA co-deposition yielded a stable coating with high reactive amino group density.

	Average number of amine groups/cm2	
	untreated	treated
EDA	(3.87 ± 0.29) x 1014	(0.52 ± 0.10) x 1014
APTES	(3.99 ± 0.44) x 1014	(4.82 ± 0.81) x 1014
APTES + EDA	(12.12 ± 0.07) x 1014	(10.04 ± 0.01) x 1014

Table 2. The surface concentration of free amine groups available for binding, calculated based on the reaction between free amines and sulfosuccinimidyl-4-[2-(4,4-dimethoxytrityl)]butyrate (sSDTB). The treated samples refer to ultrasonication for 1 minute in 1 weight % SDS solution prior to sSDTB attachment. The samples were incubated for 30 minutes in sSDTB solution, then thoroughly rinsed with water and further treated with a 37.5 % perchloric acid to allow the formation of 4,4'-dimethoxytrityl cation from the substrates. The concentration of the released cation measured by UV/vis spectrophotometer at 498 nm was used to quantify the amine group density.

Film adhesion to COP: fluorescence intensity detection

Consistent with the other measurements of reactive amine functionality, the fluorescence intensity of the APTES+-EDA co-deposited surface was the highest, and that of the APTES coated surface was significantly higher than that of the EDA

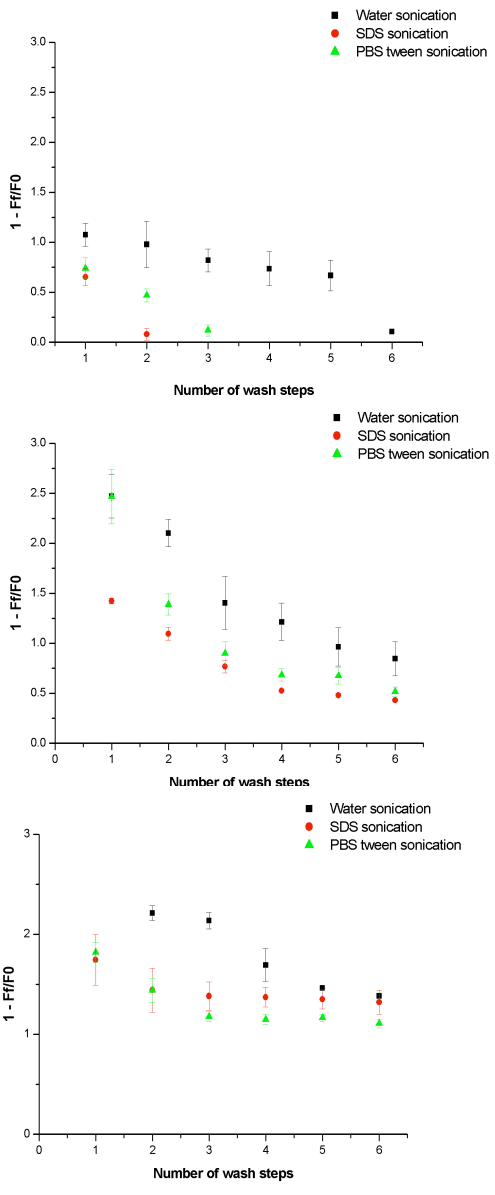

Figure 3. Fluorescence intensity variation, with washing, from lissamine™ rhodamine B sulfonyl chloride covalently bound to amine groups on (Top) EDA coated (middle) APTES coated and (bottom) APTES+EDA coated COP surface. F is the fluorescence intensity of the sample and F0 is the fluorescence intensity of the blank.

coated one (**Fig 3**). The very low fluorescence signal measured on EDA coatings can be again be associated to poor adhesion of the coating onto Zeonor®. In the case of EDA coatings, disappearance of the fluorescence intensity after 3 washing (ultrasonication) steps using SDS and PBS-Tween demonstrated a complete removal of the coating. In contrast, the fluorescence intensity stayed high on both APTES and APTES+EDA coatings demonstrating a good adhesion of the amino silane coating to the COP substrate.

ATR-FTIR spectroscopy

The presence of amine functionalities was also confirmed by ATR-FTIR spectra (see Supporting Information). The ATR-FTIR measurements taken before and after ultrasonication in water, SDS and PBS Tween (see supporting information) also demonstrated that the EDA coating was removed after sonication whereas the APTES and APTES+EDA coatings were retained. For the APTES and APTES+EDA coatings, vibration bands associated to Si-O-C and Si-O-Si vibrations were observed indicating the formation of a siloxane network.[38-40]

Film Morphology and Swelling: AFM and XRR

The interaction of the film with water was explored using AFM and XRR.. The AFM measurements carried out in air for the APTES+EDA film deposited on Zeonor® slides showed a smooth surface with a roughness of 4.51 Å (**Fig. 4 (a)**). While measured in water, the roughness increased slightly to 6.3 Å (**Fig. 4 (b)**). The surface modification on immersion in water implies water uptake of the film; this property can be quantitatively studied using XRR. Due to the strong absorption of 8 keV X-rays by water, an experimental realization using liquid water is difficult; thus, we used air saturated with H_2O (nearly 100 % humidity) to ressemble the presence of liquid water on the sample surface as water vapor and liquid water have similar chemical potentials in equilibrium conditions.

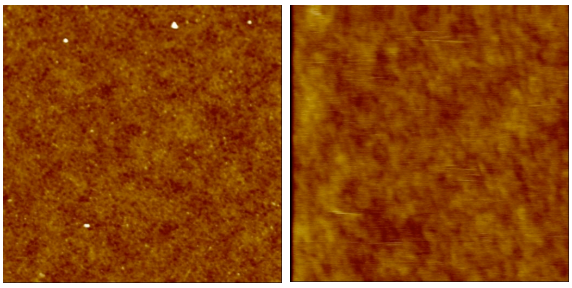

Figure 4. Atomic force microscopic image of APTES+EDA coating on zeonor slides measured in (a) air, RMS = 0.45 +- 0.01 nm and in (b) water, RMS = 0.63 +- 0.01 nm. Image size: 1 µm x 1 µm. Z-scale: 10 nm.

Fig. 5 (black squares) shows the reflectivity of a dry APTES+EDA sample measured under N2 flow. Oscillations of the reflectivity, so called Kiessig fringes, are apparent. The spacing between these fringes, Δq, can be used to estimate the film thickness, $d = 2\pi/\Delta q$. A thickness of 91 Å was estimated from data in **Fig. 5**. Changes in properties of APTES+EDA coating were observed after exposure to water vapor as shown in **Fig. 5** (red circles): The film thickness estimated from the Kiessig fringe spacing did not increase significantly (91.4 Å), but the fringes at high q were less pronounced, showing a surface roughening. Also shown in **Fig. 5** are best fits of the

reflectivity assuming a 2-layer model, accounting for a COP layer and the surface functionalization. The corresponding scattering length densities (SLD) profiles shown in the inset of **Fig. 5** reveal thicknesses of 93 Å and 94.5 Å, close to the above estimates, and surface roughnesses of 5.2 Å and 8.8 Å,

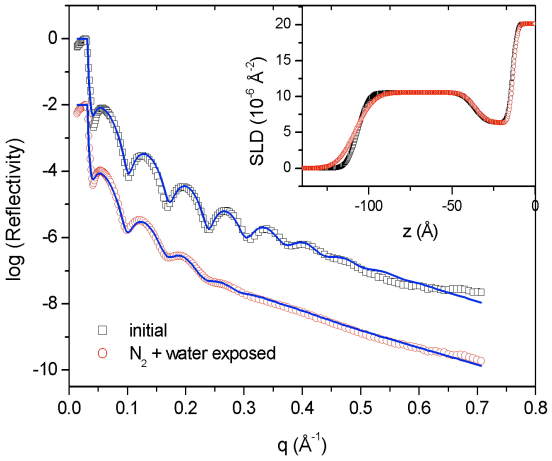

Figure 5. Specular X-ray reflectivity of an APTES+EDA sample deposited on COP spin coated on a Si (111) substrate during exposure to dry N2 (black squares) and after 45 min exposure to water vapour (red circles). The blue solid lines are best fits. The corresponding scattering length densities (SLD) are shown in the inset (black: initial, red: after water exposure)

respectively. The substrate SLD was fixed at the value for Si (2.1·10-6 Å-1). The top layer has an SLD of approximately 1·10-5 Å-1, which is close to the values for water (9.5·10-6 Å-1) and COP (~9·10-6 Å-1). Due to the similarity of the SLD values of COP and the surface functionalization, we cannot resolve two layers for the COP and surface film, especially if this interface is diffuse (rms roughness of the order of the film thickness),. The fitting requires a dip in the SLD close to the substrate that can possibly be ascribed to the norbornene group of the COP bonding to the Si substrate. The single precursor samples APTES and EDA prepared for this study (reflectivity not shown), exhibit thicknesses of 42 Å and 37 Å, respectively, i.e. all samples are within a thickness range comparable with films obtained by liquid phase silanization using APTES, reported between 7 Å up to 118 Å depending upon the nature of solvent used and the experimental conditions.[41] The fact that the single precursor samples are thinner than the estimated initial COP layer (~70 Å) shows that the argon + oxygen plasma pre-treatment before deposition removes a significant fraction of the COP.

For in-situ observation of changes during water vapor exposure and N_2 drying, the reflectivity was continuously scanned over a small q-range between 0.01 and 0.15 Å-1 . Selected curves are shown in **Fig.6 a**. The curves labeled with negative times were measured under dry N_2 stream, and the water vapour was added at t=0. For the fitting in the limited q-range, the parameters obtained from the fits in Fig. 5 were used as starting values, and only the thickness of the two layers and the roughness of the topmost layer were allowed to vary. SLD profiles are plotted in the right column of **Fig. 6 a**, and due to the limited q-range used for fitting need to be interpreted qualitatively. The changes in film thickness and roughness as determined from the fitting parameters are shown in **Fig.6 b**. It is noteworthy that considerable roughening occured, from 5.1 Å to 8.9 Å, during exposure to

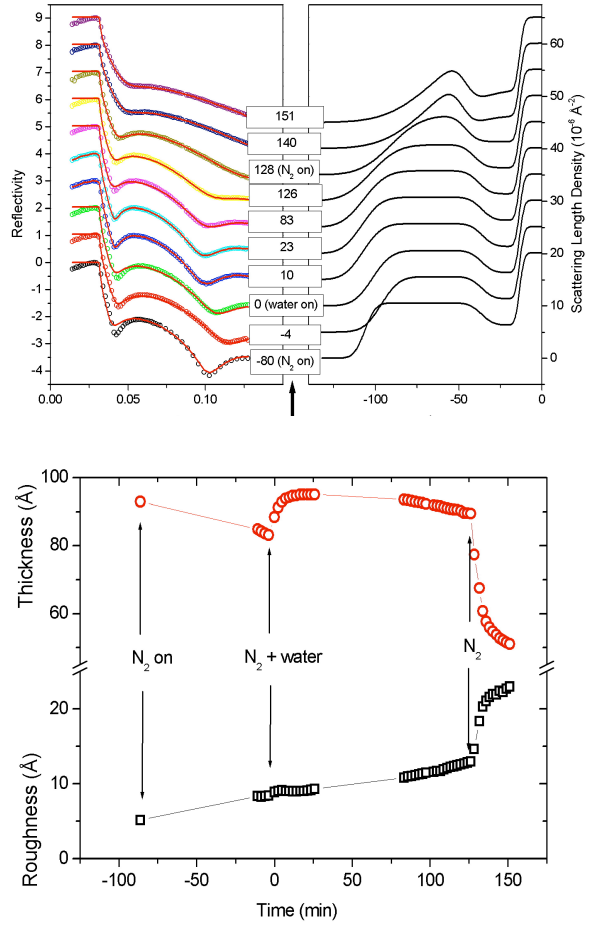

Figure 6. (Top) In-situ reflectivity (symbols) measured during exposure to N2 (t < 0 min and t > 128 min) and water vapour (0 min < t < 128 min) (left) and corresponding best fits (red solid lines). The times of exposure are indicated. The right column shows the calculated SLD profiles. (Bottom) Film thickness obtained from the fits to the in-situ reflectivity curves. The dashed curves are guides to the eye.

dry N_2, accompanied by a decrease in film thickness from 93 Å to 83 Å.. On exposure to water vapor, a rapid increase in film thickness, to 95 Å , followed by a slight decrease to 89 Å occurs, while further roughening to 13 Å after longer exposure was observed, with no significant change in the rate of roughening after adding water vapor. At t = 128 min, the input was again changed back to N_2, and a rapid decrease in thickness to 51 Å and rapid further roughening to 23 Å was observed. ..

Nanoparticle approach to study the film reactivity

AFM images of the nanoparticle distribution on untreated Zeonor® surface and on the plasma deposited coatings are

presented in **Fig. 7**. The number and distribution of NPs deposited on each slide reflect the relative distribution of amine groups available on the external surface to react with objects as large as nanoparticles. The relative reactivity revealed by this method was somewhat different to that obtained from the colorimetric method. The NP concentration attached to the APTES coating was 95 % higher than that attached to the EDA coating, and the amount attached to the APTES+EDA coating was higher still.

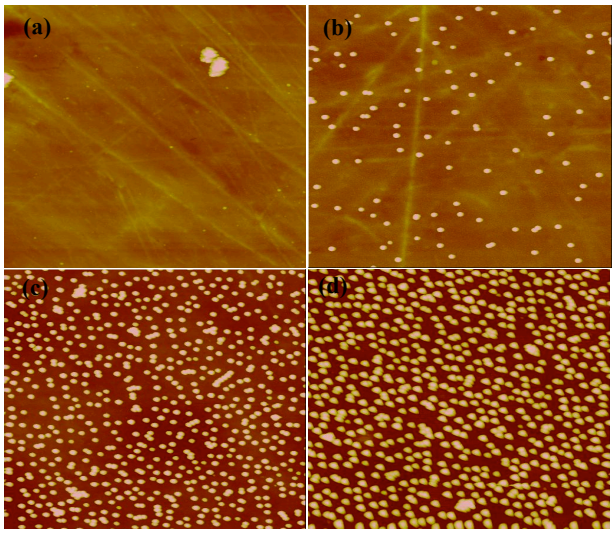

Figure 7. Tapping-mode™ AFM images of (a) untreated, (b) EDA coated, (c) APTES coated (d) and APTES+EDA coated COP surface, showing the distribution and density of the covalently bound nanoparticles.

Application in biosensor platforms assessing non-specific binding

The applicability of such coatings for biosensor platforms was demonstrated through oligonucleotide attachment. A short, 15 base oligonucleotide strand modified with fluorescein on the 3'-end and with an amino-group at the 5' terminus was covalently (specific binding) immobilized on both APTES and APTES+EDA coated COP slides via a homofunctional bilinker. In parallel, a second set of APTES and APTES+EDA coated slides were prepared, and subsequently capped with blocking reagent to allow only non-covalent (non-specific) immobilization of the ssDNA The average oligonucleotide binding signals, obtained by measuring the fluorescence intensities of each slide, are summarized in **Fig. 8**. The covalent attachment of the ssDNA (filled circle and triangle) was significantly higher than its non-specific binding (empty circle and triangle) on the capped slides.

The assay detection limit and its sensitivity are largely determined by the amount of non-specific binding. Therefore, the surface fidelity, presented here as the ratio between the specific and non-specific binding at various DNA concentrations was calculated and shown in **Table 3**.

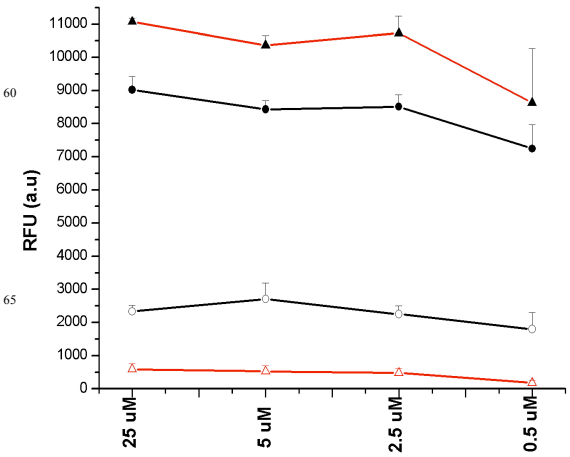

Figure 8. Plot illustrating the binding capacity of APTES (black) and APTES + EDA (red) coated cyclic olefin polymer surfaces. Fluorescein labeled oligonucleotide was immobilized on the amino functionalized slides via homofunctional bilinker. Specific (solid) and non-specific (hollow) binding of ssDNA was measured by means of fluorescence. The blocking reagent used to cap slides to assess the amount of non-specific binding was Tris(hydroxymethyl)aminomethane.

Surface Chemistry		Surface fidelity [a]			
1st layer	2nd layer	25 µM	5 µM	2.5 µM	0.5 µM
APTES	PDITC	3.9	3.1	3.8	4.0
APTES + EDA	PDITC	19	19.3	21.9	46.5

Table 2. Surface fidelity presented as the ratio between the specific and non-specific binding at various DNA concentrations. [a] Calculated as a ratio between the relative fluorescence units of unblocked over blocked slides at various DNA concentrations

Discussion

The high resolution XPS scan of C 1s core level photo emission spectra (**Fig. 2**) showed that the relative amount of C-N bonding was higher in APTES+EDA than the APTES and EDA on its own, **Table 1**. Also the elemental analysis revealed that the atomic percentage of nitrogen (N 1s) was higher for APTES+EDA than APTES. Although the atomic percentage of nitrogen was higher in EDA, the coating adhesion to Zeonor® was poor and the amine contents decreased after SDS sonication, as shown in **Fig. 3a**. These two facts demonstrate that the APTES+EDA deposition results in higher amount of amine groups than the APTES.

The relative results of XPS for the APTES and APTES+EDA coatings are consistent with the inference from sSDTB reaction regarding the relative concentration of reactive groups in the coating. The number of reactive amino groups per cm² measured, using the colorimetric sSDTB reaction, for the APTES and APTES+EDA coatings remained essentially unchanged after the detergent sonication procedure, Table 2. However, for the EDA coatings the number of amine groups per cm^2 decreased sharply after detergent sonication. This

observation can be interpreted as a very poor adhesion of the EDA coating on COP substrates. Overall, the colorimetric measurement using sSDTB showed that APTES + EDA co-deposition yielded a stable coating with high reactive amino group density.

The disappearance of fluorescence intensity, from covalently attached lissamine fluorophore, after 3 washing (ultrasonication) steps using SDS and PBS-Tween on the EDA coated slides demonstrated a complete removal of the coating (**Fig. 3a**). A higher bound fluorescence intensity for the APTES+EDA coatings demonstrates the presence and reactivity of higher amounts of amine groups on the APTES+EDA coated surfaces (**Fig. 3c**) and the enhancement in stability of the surface obtained as a result of the use of silane reagent in the plasma.

A schematic for the reaction mechanism is presented in **Fig. 9** The picture that emerges from the different characterizations is the formation of a weak hydrogen bonded coating containing amine functionalities from EDA deposition (**Fig 9a**) that could easily be washed away with a detergent and the formation of a siloxane-silicone network in APTES and APTES+EDA deposition, that carries aminated side chains (**Fig 9b** and **9c**) The siloxane-silicone a network could be formed by fragmentation of APTES into aminosiloxane radicals that condense and polymerise on the surface. If these radicals are further fragmented (unpublished data: the amine functionality decreased with higher input RF power and longer deposition time), or the siloxane functionality is not present, then a stable, adherent, amine-reactive network is not formed on COP. The siloxane functionality seems essential both for insertion into C-C bonds of the COP substrate and for building a stable, polymerized network.

formed a stable coating with silica-like properties on COP, that was a suitable surface for the construction of lateral flow bio assay chips.29,30

The siloxane networks in APTES and APTES+EDA films, as observed in ATR-FTIR, were necessary for stable film formation on cyclo olefinic copolymers. Also the presence of EDA along with the aminated siloxane enhanced the amine content in the resultant film. In the presence of EDA, the resultant alkylamine radicals present in the plasma could insert into the alkylated siloxane network to increase the reactive amine functionality (**Fig 9c**).

Film morphology is one of the factors that cause non specific biomolecule binding provided the surface roughness is comparable to or larger than the size of the biomolecule to be immobilized.[42-44] A higher surface roughness implies an increased surface area that could increase the physisorption of the biomolecule as the molecule could stretch out on the rough surface. It has been reported that films with roughness ranging from micrometer to nanoscale (>5nm) enhance adsorption of proteins.[45,46] For the immobilization of DNA and also for the ultrasensitive detection of DNA, a surface with a roughness of 5 Å has been used.[47,48]

The observed initial surface roughness of 5.2 Å for the APTES+EDA films (**Fig. 6 right**) is comparable with that found for films formed from liquid phase silanization using APTES on silica, mica and glass surfaces.[49-51] Two different processes are likely to account for the shrinking of the film during drying (**Fig. 6b**, t<0), the evaporation of residual, unreacted EDA and the evaporation of trapped water absorbed from ambient atmosphere. EDA does not covalently bond to the COP groups (**Fig. 9a**), and is volatile at room temperature.

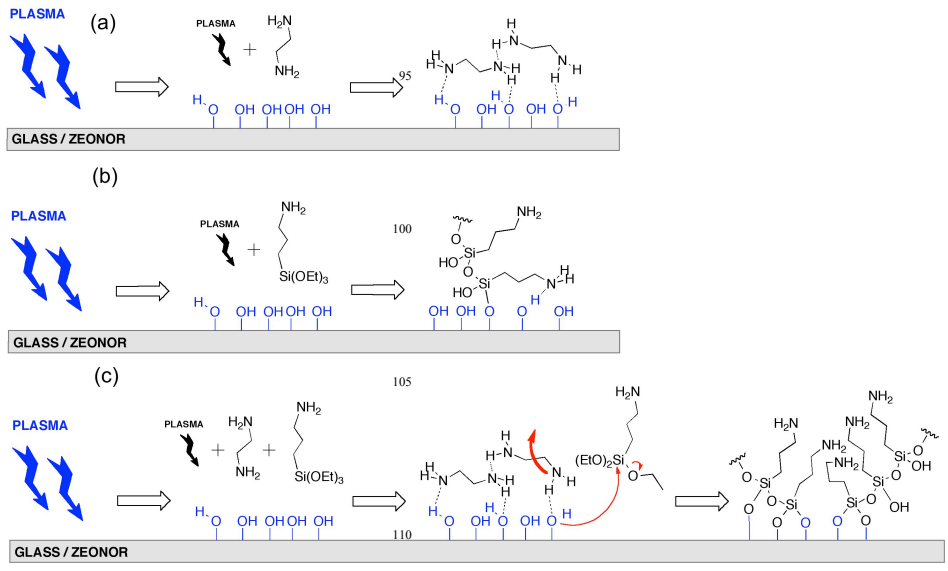

Figure 9. Proposed reaction mechanism of EDA (a), APTES (b) and APTES+EDA (c) to Zeonor®.

It has been demonstrated earlier that the siloxane network formed using hexamethyldisiloxane as precursor for PECVD

The rapid swelling during exposure to water vapor (t>0 in **Fig. 6**) shows that the film is highly hygroscopic; thus, it is

reasonable to assume that it already has taken up moisture during exposure to ambient conditions. It should be noted that pure COP does not absorb water[52] and the film hygroscopicity arises solely from the surface functionalization. The water uptake likely occurs by hydration of internal hydrogen bonds of amine groups with the siloxane and siloxyl groups of the silane/siloxane network, of the unreacted EDA and of amides that may have been formed during deposition. This hydration is responsible for the observed volume expansion. In the drying process of this high water content network, the hydrated bonds are broken, causing volume contraction, and new hydrogen-bonds are formed, with an associated increase disorder resulting in an irreversible increase in surface roughness. This process also facilitates further loss of EDA which is reflected in the continuing decrease in film thickness. The observed increase in roughness in the drying process is in contrast with the water uptake stage, where the existing bonds are hydrated and the disorder is not increased. Hence, the roughness does not increase significantly, but only slightly due to the exchange of water during vapor exposure. The AFM images shown in **Fig. 4** do not involve a drying process, and the increase in roughness from 0.45 nm to 0.63 nm is only moderate, comparable to the water vapor exposure stage in **Fig. 6**.

Although the roughness increased irreversibly, the roughness variation on exposure to water vapour and drying from 5.1 to 23 Å is within the range reported experimentally that allows covalent immobilization of DNA and proteins.[53,54] The washing and sonication experiments showed a stable residual film, and the observed processes during water interaction and drying only modify the non-covalently bound parts of the surface functionalization.

The nanoparticle method shows the density of reactive groups at the external surface (**Fig. 7**): reactive groups within the interior of a coating that might be swollen in contact with the solution could be accessible to a molecular probe but are not accessible to a probe of the size of a nanoparticle. Although the nanoparticle distribution cannot directly reveal the amount of amine groups on the surface, it does provide an idea of their density, distribution and their capability to bind nano objects. It proved to be a very useful and rapid tool for qualitative assessment of the reactive amine content of the film surface, revealing, for example, that excessive plasma power destroyed the reactive amine functionality in the coating. The NP coupling chemistry was constant and surfaces with varying amounts of amine functional groups showed a relevant variation in the quantity of covalently bound NPs.

The ssDNA attachment data (**Fig. 8**) illustrate that the blocking reagent acts more efficiently on the APTES+EDA coatings rather than APTES, thus reducing the non-specific adsorption of the ssDNA. In general, the higher the signal / noise ratio, the lower limits of detection can be achieved. At all measured DNA concentrations in **Table 3**, APTES + EDA coatings showed significant improvement in surface fidelity when compared to APTES coated COP slides. Therefore, the functionalized surface binds oligonucleotides through a combination of mostly covalent and to some extent also non-covalent interactions. Such simple experiments provided further evidence that the co-deposition of APTES+EDA leads to the formation of surfaces with high homogeneity and amino group density available for binding of biorecognition elements, which makes the PECVD technique a very attractive method to prepare reactive surfaces for bioassay devices.

Conclusion

We have successfully created amino functional coatings on COP substrates by PECVD. The surface chemical and physical characteristics including the chemical composition, homogeneity, stability, reactivity and morphological properties has been characterized. We found that the siloxane functionality is essential to create a stable, adherent amine reactive network on COP substrates. The application of such surfaces to biomolecule binding has been demonstrated. Alteration of the precursor composition, in this case the use of mixtures of APTES and EDA, altered favorably the surface adhesion, the concentration and availability of reactive amine groups and the ratio of specific to non-specific binding of surfaces functionalized with bio-active receptors. These findings demonstrate a general approach showing a route to introduce different functionalities by choosing alkoxy-silane precursors with the desired functionality. As the PECVD process is suitable for bulk processing and is environmentally friendly, the amine functionalisation of COP platforms using the methodology mentioned in this paper could potentially be used for bulk industrial processing of biosensor devices. As a first step towards application of this method, we have successfully demonstrated surface activation of a next-generation commercial prototype, a microfluidic chip made of COP, obtained from Amic AB (Uppsala, Sweden) (supplementary information). The further exploration of the use of different feed vapor compositions, and the optimization of power, coating time and plasma geometry, offer much scope for development of this fast and efficient method for surface activation of polymer bio-devices. Moreover, because PECVD is a gas phase based deposition, this methodology can be used to introduce functionalities into microcavities such as pre-assembled microfluidic chips, which is still a challenge in the development of functional microfluidic devices.

Acknowledgments

This material is based upon work supported by the Science Foundation Ireland under Grant No. 05/CE3/B754. Cedric Volcke is a postdoctoral researcher of the Belgian Fund for Scientific Research (F.R.S. / F.N.R.S.). D.E.Williams is an E.T.S. Walton Visiting Fellow of Science Foundation Ireland. Portions of this research were carried out at the Stanford Synchrotron Radiation Lightsource, a national user facility operated by Stanford University on behalf of the U.S.

Department of Energy, Office of Basic Energy Sciences.

Notes and references

[a],* *Biomedical Diagnostics Institute (BDI) Dublin City University, Collins Avenue, Glasnevin, Dublin 9, Ireland. Fax: +353 1 7006558; Tel: +353 1 7007984; Email: ramprasad.gandhiraman@dcu.ie*
[b] *Research Centre in Physics of Matter and Radiation (PMR), University of Namur (FUNDP), 61, rue de Bruxelles, B-5000 Namur, Belgium.*
[c] *Research Centre for Surface and Materials Science, Department of Chemical and Materials Engineering, University of Auckland, Private Bag 92019, Auckland 1142, New Zealand*
[d] *Industrial Research Limited, 69 Gracefield Road, P.O. Box 31-310, Lower Hutt 5040, New Zealand*
[e] *Stanford Synchrotron Radiation Lightsource, 2575 Sand Hill Road, Menlo Park, California 94025, USA.*
[f] *National Centre for Plasma Science and Technology, Dublin City University,Collins Avenue, Glasnevin, Dublin 9, Ireland*
[g] *MacDiarmid Institute for Advanced Materials and Nanotechnology, Department of Chemistry,University of Auckland, Private Bag 92019, Auckland 1142, New Zealand.*

† Electronic Supplementary Information (ESI) available: Detailed experimental details and additional results are provided. See DOI: 10.1039/b000000x/

1. M.J. Pugia, G. Blankenstein, R.P. Peters, J.A. Profitt, K. Kadel, T. Williams, R. Sommer, H.H. Kuo, L.S. Schulman, *Clinical Chemistry* 2005, **51:10,** 1923-1932.
2 H. Xu, J.R. Lu, D.E. Williams, *J. Phys. Chem. B* 2006, **110,** 1907-1914.
3 S. Boujday, A. Bantegnie, E. Briand, P.G. Marnet, M. Salmain, C.M. Pradier, *J. Phys. Chem. B* 2008, **112**, 6708-6715.
4 M. Vareiro, I. Tranchant, S. Maplin, K. Zak, M.M. Gani, C.J. Slevin, H.C. Hailes, A.B. Tabor, P.J. Cameron, A.T.A. Jenkins, D.E. Williams, *Anal. Biochem.* 2008, **377,** 243-250.
5 M. L. M.Vareiro, J. Liu, W. Knoll, K. Zak, D.E. Williams, A.T.A. Jenkins, *Anal. Chem*. 2005, **77,** 2426-2431.
6 S.G. Im, K.W.Bong, B.S. Kim, S.H. Baxamusa, P.T. Hammond, P.S. Doyle, K.K. Gleason, *J. Am. Chem. Soc*. 2008, **130 (44),** 14424–14425.
7 M.H.Lin, C.F. Chen, H.W. Shiu, C.H. Chen, S. Gwo, *J. Am. Chem. Soc.* 2009, **131 (31),** 10984–10991.
8 G.A. Diaz-Quijada, R. Peytavi, A. Nantel, E.Roy, M.G. Bergeron, M.M. Dumoulin, T.Veres, *Lab Chip.* 2007,**7,** 856-862.
9 J. Kameoko, H.G. Craighead, H. Zhang,. J. Henion, *Anal. Chem.,* 2001,**73,** 1935-1941.
10 A. Bhattacharyya, C. M. Klapperich, Lab Chip. 2007,7, 876-882.
11 C. Jonsson, M. Aronsson, G. Rundstrom, C. Pettersson, I. Mendel-Hartvig, J. Bakker, E. Martinsson, B. Liedberg, B. MacCraith, O. Ohman, J. Melin, *Lab Chip.* 2008, **8,** 1191-1197.
12 S. Laib, B.D. MacCraith, *Anal. Chem.* 2007, **79,**6264-6270.
13 J. Raj, G. Herzog, M. Manning, C. Volcke, B.D. McCraith, S. Ballantyne, M. Thompson, D.W.M. Arrigan, *Biosen & Bioelectron.* 2009, **24,** 2654-2658.
14 J.C. Hicks, R. Dabestani, A.C. Buchanan, C.W. Jones, *Chem. Mater.* 2006, **18,** 5022-5032.
15 J.C. Hicks, R. Dabestani, A.C. Buchanan, C.W. Jones, *Inorg. Chim. Acta* 2008,**361,** 3024-3032
16 J.C. Hicks, C.W. Jones, *Langmuir* 2006, **22,** 2676-2681.
17 S.A. Kanan, W.T.Y. Tze, C.P. Tripp, *Langmuir* 2002, 18, 6623-6627.
18 S Roy.. X. Chen, M.H. Li, Y. Peng,F. Anariba, Z. Gao, *J. Am. Chem. Soc*. 2009, **131 (34),** 12211–12217.
19 G. Hilton, P. Lewis, D.J. Edell, K.K. Gleason, *Chem. Mater.* 2000, **12 (11),** 3488–3494
20 L.D. White, C.P. Tripp, *J. Colloid Interface Sci.* 2000, **232,** 400-407.
21 M. Arroyo-Hernandez, J. Perez-Rigueiro, A.Conde, A.Climent, R.Gago, M. Manso, J. M. Martinez-Duart, *J. Mater. Res.* 2008, **23,** 1931-1939.
22 A. Anderson, W.R. Ashurst, *Langmuir* 2008, **24,** 7947-7954.
23 P. Favia, M. Creatore, F. Palumbo, V. Colaprico, R.d'Agostino, *Surf. Coat. Technol.* 2001,**142-144,** 1-6.
24 H. Muguruma, Y.Kase, *Biosens. Bioelectron.* 2006, **22,** 737–743.
25 R. Di Mundo, M. Ricci, R.d'Agostino, F.Fracassi, F. Palumbo, *Plasma Process. Polym.* 2007, **4,** S21-S26.
26 D. Jung, S.Yeo, J. Kim, B. Kim, B. Jin, D.Y. Ryu. *Surf. Coat. Technol.* 2006, **200,** 2886-2891.
27 K. Nakanishi, H.I. Muguruma, I. Karube, *Anal.Chem.* 1996, **68,** 1695-1700.
28 J. Kim, D. Jung, Y. Park, Y. Kim, D.W. Moon, T.G. Lee, *Appl. Surf. Sci.,* 2007, **253,** 4112- 4118.
29 M.M. Dudek, R.P. Gandhiraman, C. Volcke, A.A. Cafolla, S. Daniels, A.J. Killard, *Langmuir* 2009, **25(18),** 11155-11161.
30 M.M. Dudek, R.P. Gandhiraman, C. Volcke, S. Daniels, A.J. Killard, *Plasma. Process. Polym.* 2009, **6,** 620-630.
31 R.P. Gandhiraman, S.K. Karkari, S.M. Daniels, B.D. MacCraith, *Surf. Coat. Technol.* 2009, **203,** 3521-3526.
32 F.J.Arriagada, K. Osseo-Asare,. *J. Colloid Interface Sci.* 1999, **211,** 210-220.
33 M. Tolan, *X-Ray Scattering from Soft-Matter Thin Films: Materials Science and Basic Research,* Berlin; New York: Springer-Verlag Telos, 1999
34 O. Heavens, *Optical Properties of Thin Films.* London: Butterworth. 1955
35 A. Nelson, *J. Appl. Crystallogr.* 2006, **39,** 273-276
36 G. Beamson, D. Briggs, *High resolution XPS of organic polymers: The Scienta ESCA300 Database,* John Wiley & Sons, Chichester, 1992.
37 R.K. Gaur, K.C. Gupta, *Anal Biochem.* 1989, **180,** 253-258.
38 D.G. Kurth, T. Bein, *Langmuir* 1995, **11,** 3061-3067.
39 P. Innocenzi, *J. Non-Cryst. Solids,* 2003, **316,** 309-319.
40 M. Minier, M. Salmain, N. Yacoubi, L. Barbes, C. Methivier, S. Zanna, C.-M. Pradier, *Langmuir* 2005, **21,** 5957-5965.
41 R.M. Pasternack, S.R. Amy, Y.J. Chabal, *Langmuir* 2008, **24 (22),** 12963–12971
42 M. Advincula, X. Fan, J. Lemons, R. Advincula, *Colloids Surf. B: Biointerfaces,* 2005, **42,** 29-43
43 K. Rechendorff, M.B. Hovgaard, M. Foss, V.P. Zhdanov, F. Besenbacher, *Langmuir* 2006, **22,** 10885-10888
44 B. Wälivaara, B.O. Aronsson, M. Rodahl, J. Lausmaa, P. Tengvall, *Biomaterials* 1994, **15,** 827
45 J.M. Wen, A.J. Ruys, R.S. Mason, P.J. Martin, A. Bendavid, Z. Liu, M. Ionescu, H. Zreiqat, *Biomaterials* 2007, **28,**1620.
46 K. Rechendorff, M.B. Hovgaard, M. Foss, V.P. Zhdanov, F.Besenbacher, *Langmuir* 2006, **22,** 10885-10888
47 D. Liu, A. Bruckbauer, C. Abell, S. Balasubramanian, D.-J.Kang, D. Klenerman,D. Zhou, *J. Am. Chem. Soc.,* 2009, **131 (34),** 12211–12217.
48 S. Roy, X. Chen, M.-H. Li, Y. Peng, F. Anariba, Z. Gao, *J. Am. Chem. Soc*. 2006, **128 (6),** 2067–2071
49 J. Hu, M. Wang, H.-U.G. Weier, P. Frantz, W. Kolbe, D.F. Ogletree, M. Salmeron, *Langmuir* 1996, **12 (7),** 1697–1700
50 R.M. Pasternack, S.R. Amy, S.R.; Chabal,Y.J. *Langmuir* 2008, **24 (22),** 12963–12971
51 A, Kasry, P. Borri, P.R. Davies, A. Harwood, N. Thomas, S. Lofas, T. Dale, *Appl. Mater. Interfaces,* 2009, **1 (8),** 1793–1798.
52 M.Yamazaki, *J. Mol. Catal. A: Chem.* 2004, **(213),** 81–87
53 K. Arinaga, U. Rant, M. Tornow, S. Fujita, G. Abstreiter, N. Yokoyama, *Langmuir* 2006, **22 (13),** 5560–5562.
54 A. Bhaumik, M. Ramakanth, L.K. Brar, A.K. Raychaudhuri, F. Rondelez, D. Chatterji, *Langmuir* 2004, **20 (14),** 5891–5896.